STUDY OF MICRO-DISCHARGES IN DIELECTRIC BARRIER DISCHARGE: INFLUENCE OF ELECTRODE STRUCTURE AND MATERIALS

Manish Pandey 1 *, Manoj Khadka2, Bhesh Bahadur Thapa3, Raju Bhai Tyata3

¹ Department of Physics, St. Xavier's College, Tribhuvan University ² Department of Physics, Khwopa College, Tribhuvan University

Abstract

For the electrical characterization of Dielectric Barrier Discharge (DBD) at atmospheric pressure, various electrode systems were utilized. DBD was generated in air under atmospheric conditions and powered by a high AC voltage and high-frequency power supply. The current-voltage characteristics were analyzed for electrode gaps of 2 mm and 3 mm, varying the voltage from 0 to 12 kV while maintaining a frequency of 20 kHz for each electrode type (disk, cylindrical, and double cylindrical). In general, the number of micro-discharges (filaments) increased with rising voltage in each cycle. Notably, a stable glow discharge was observed in the double cylindrical electrode system at a 2 mm gap as the voltage varied. This configuration proved to be efficient, with the average power consumption being only one-third that of the single cylindrical electrode at the same gap. The energy dissipation for this system was calculated to be 18.25 μJ using power analysis and 16.74 μJ using the I-V characteristic curve.

Keywords: Plasma, DBD, Micro-discharges, Electrical Characterization

1. Introduction and Background

Dielectric Barrier Discharge (DBD) is a non-equilibrium electrical discharge created between two electrodes using a high-voltage power supply. In DBD, a dielectric material covers at least one of the electrodes, which serves as a current limiter and prevents the formation of sparks or arcs. Siemens (1857) first introduced this concept, which has since led to the widespread use of common dielectric materials such as glass, quartz, ceramics, plastic films, and silicon rubber.

At atmospheric pressure, non-equilibrium plasma generated by DBD exhibits electron temperatures much higher than those of heavy particles. Because of the high frequency of collisions between electrons and heavy particles, electrons lose energy at a rapid rate, making it difficult to ob-

*Corresponding author: Manish Pandey Department of Physics, St. Xavier's College, Maitighar, Kathmandu Email: manish.phy.math@gmail.com (Received: Jan. 17, 2025, Accepted: April 11, 2025) https://doi.org/10.3126/jsce.v12i1.78349 tain a stable plasma. Although DBD systems often operate in filamentary mode at atmospheric pressure, they can also achieve a diffuse mode under specific conditions, allowing spatial homogeneity and making them suitable for applications such as homogeneous surface treatments (Kogelschatz, 2002; Wang and He, 2006).

Several studies have examined the behavior of DBD systems under varying conditions. For instance, Tyata et al. (2010) investigated DBD discharges with electrode gaps of 1 mm and 2 mm, reporting filamentary discharges with dielectric materials and glow discharges without them. Similarly, Jabur et al. (2020) identified 4 mm as the optimal electrode separation for efficient plasma generation in DBD systems. Singh et al. (2024) demonstrated that a 3 mm discharge width minimizes power consumption in atmospheric pressure DBD reactors, highlighting the importance of achieving an optimal balance between discharge width and input voltage. Furthermore, Subedi and Tyata (2010) compared three electrode configurations: cylindrical, parallel plate and annular systems, finding that the most stable

³ Department of Sciences and Humanities, Khwopa College of Engineering, Tribhuvan University

discharge was produced using the parallel plate electrode system. These findings collectively underscore the importance of exploring various electrode configurations and gap sizes to optimize the performance and efficiency of DBD systems for diverse applications.

Although DBD systems typically operate with discharge gap spacings ranging from 0.1 mm (e.g., in plasma displays) to about 1 mm (e.g., in ozone generators) (Foest et al., 2006), there is limited research on the effects of larger gap distances on plasma properties and stability. Current studies also lack a comprehensive understanding of how different electrode designs and materials influence discharge behavior, especially at larger gap distances.

To address this gap, this study investigates different electrode systems with gap distances of 2 and 3 mm, aiming to identify optimal conditions for achieving stable glow discharges suitable for diverse plasma applications. The primary objective of this study is to investigate how variations in electrode gap, voltage, and system design influence the properties and stability of plasma generated by DBD.

The materials and configurations of the electrodes play a critical role in defining the behavior of DBD plasma. As emphasized by Wang et al. (2012), understanding these relationships is crucial for optimizing DBD systems for specific applications, such as surface treatments, water purification, and material processing. This study contributes to the existing knowledge base by systematically characterizing the effects of different electrode systems on plasma behavior.

This paper evaluates the micro-discharges generated by DBD systems in air and power analysis, using three different electrode materials and configurations. We systematically investigate the influence of electrode design and gap size, aiming to determine the optimal combination of parameters to achieve stable and efficient plasma discharges.

2. Experimental Details

The experimental setup and its electrical connections are depicted in Figure 1, with a corresponding photograph presented in Figure 2. For the experiment, we utilized a high-frequency, high-voltage power supply (PVM500) and its corresponding driver (DIDRIVE10). This power supply allows an adjustable voltage in the range of 0–20 kV and a frequency between 10–30 kHz. Specifically, for the generation of DBD, we supplied 0–12 kV AC at 20 kHz. In addition, we developed three specialized electrode systems, which are shown in Figure 3, with their photographs shown in Figure 4. We studied electrical characterization with the help of a high-voltage probe using the OWON digital oscilloscope model DS 7102.

The experimental arrangement remained consistent across all three electrode systems, with the only variation being the type of electrode used. In the case of the double

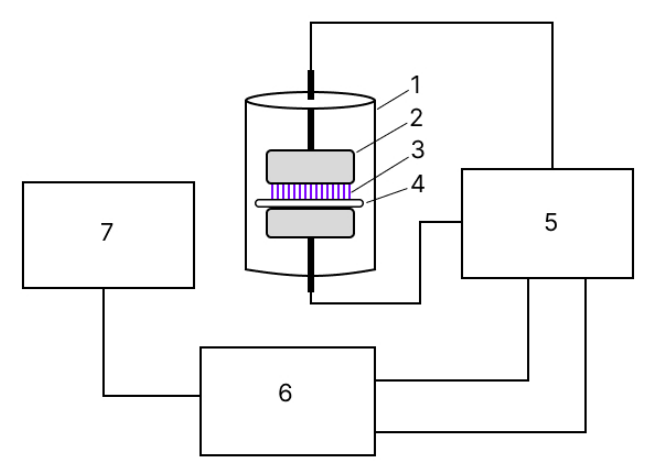


Figure 1. Schematic diagram of the experimental set-up and measurement connection: 1-transparent holder, 2-electrode, 3-micro discharges, 4-glass plate, 5-plasma driver with probe, 6-oscilloscope, 7-computer.



Figure 2. Experimental set-up of the disc electrode system, which produced discharge using high voltage and high-frequency power supply at atmospheric pressure.

cylindrical electrode system, the openings oriented in the same direction were connected together to form a unified electrode structure. This design ensured uniform operation and facilitated effective experimentation with the different electrode configurations. The setup was carefully calibrated to minimize potential errors and ensure accurate measurements during testing.

2.1. Electrode Design

2.1.1 Disk Electrode

The disk electrode system comprises two identical circular copper disc electrodes, each with a diameter of 50 mm and a thickness of 5 mm. These electrodes are arranged parallel to each other, ensuring symmetry in the setup. When an AC voltage is applied, a filamentary dielectric barrier discharge (DBD) is generated in the air. To prevent point arcs that could damage the electrode surfaces, the discs are carefully designed with smooth surfaces. The lower disc electrode is securely fixed, while the upper electrode is adjustable, allowing fine-tuning of the gap between the discs in increments of 0.5 mm. A dielectric barrier, consisting

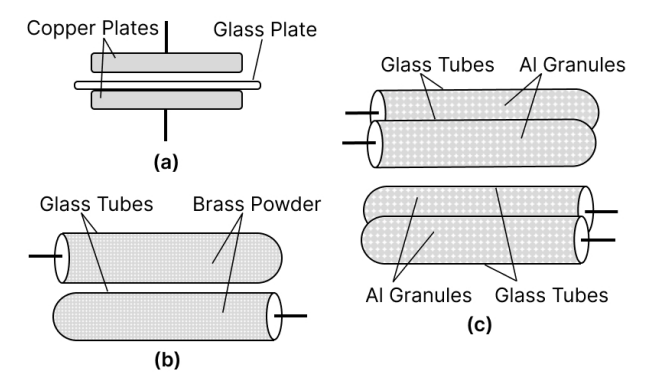


Figure 3. Schematic diagram of electrode systems: (a) Disk electrode system, (b) Single cylindrical system, (c) Double cylindrical system.

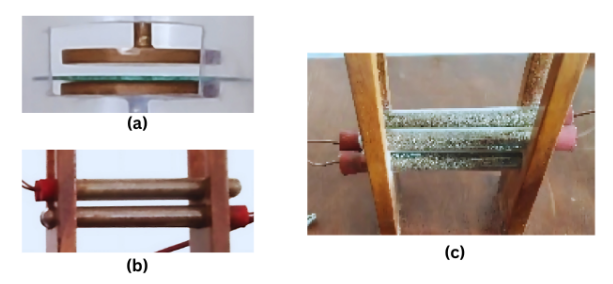


Figure 4. Electrode Images: (a) Disk electrode system, (b) Single cylindrical system, (c) Double cylindrical system

of a glass plate with a thickness of 1 mm, is positioned between the electrodes to stabilize the discharge and prevent arcing.

2.1.2 Single Cylindrical Electrode

The single cylindrical electrodes are fabricated using a glass tube made of durable borosilicate material, measuring 100 mm long and having an inner diameter of 12 mm. The tube is filled with finely powdered brass, and a thin copper wire is inserted coaxially within the packed material. The ends of the glass tube are sealed with cork to keep the powder in place and ensure stability. These cylindrical electrodes are mounted horizontally on an insulating wooden stand, with one electrode fixed in position while the other is movable. The movable electrode facilitates precise adjustment of the gap between the electrodes, enabling controlled experimentation and ensuring consistent discharge characteristics.

2.1.3 Double Cylindrical Electrode

The double cylindrical electrode system is constructed using borosilicate glass tubes, each measuring 100 mm in length and 12 mm in diameter. The tubes are filled with aluminum granules, and a thin copper wire is coaxially em-

bedded within the packed material. The openings of the tubes are sealed with cork to secure the aluminum granules. Two such electrodes are mounted horizontally on an insulating wooden stand arranged parallel to each other. The lower electrode remains fixed, while the upper electrode is designed to be movable, allowing the adjustment of the gap between them. This configuration ensures flexibility in the electrode spacing, enabling the study of discharge characteristics under various experimental conditions.

3. Result and Discussion

3.1. Micro-discharge Analysis

The graph between discharge voltage and discharge current vs. time is analyzed in each case of electrodes, varying the electrode gap. The oscilloscope was used to record the voltage and current waveforms of air discharge as a function of time, while the applied voltage was manually adjusted. The observed phase difference between the voltage and current waveforms in each graph suggests a complex interplay of resistive, capacitive, and inductive plasma characteristics, consistent with previous findings by Lieberman and Lichtenberg (1994).

Across all cases of disk, cylindrical, and double cylindrical electrode systems, two key phenomena were consistently observed. First, non-uniform discharges appeared as sharp spikes in the current-time curve (red) whenever the voltage across the plasma transitioned between phases. Second, as the applied voltage increased, the number of microdischarges consistently rose. However, when the electrode gap was increased to 3mm, the number of micro-discharges decreased, aligning with Paschen's law (as evident in the Disk & Single-Cylindrical Electrode system). These findings highlight the interplay between electrode geometry, voltage, and gap size in determining discharge behavior.

For the disk electrode system, as shown in Figure 5 (a-c) and Figure 6 (a-c), there were more spikes or more irregular (non-homogeneous) discharges compared to the cylindrical electrode system, as shown in Figure 7 (a-c) and Figure 8 (ac) for discharge gaps of 2 mm and 3 mm. This suggests that the disk electrode geometry influences the uniformity of the discharge, leading to a greater degree of non-homogeneity in the current vs. time curves. In the case of double cylindrical electrode system specifically, at a 2 mm gap, increasing the peak-to-peak voltage from 1.1 kV to 1.2 kV and then to 1.3 kV caused a significant rise in the peak-to-peak current, from 4.2 mA to 6.2 mA to 7.4 mA, as shown in Figure 9 (a-c). Under these conditions, the micro-discharges remained uniform, as indicated by the red curve. In contrast, at a 3 mm gap, the micro-discharges became irregular and non-uniform, as shown in Figure 10 (a-c).

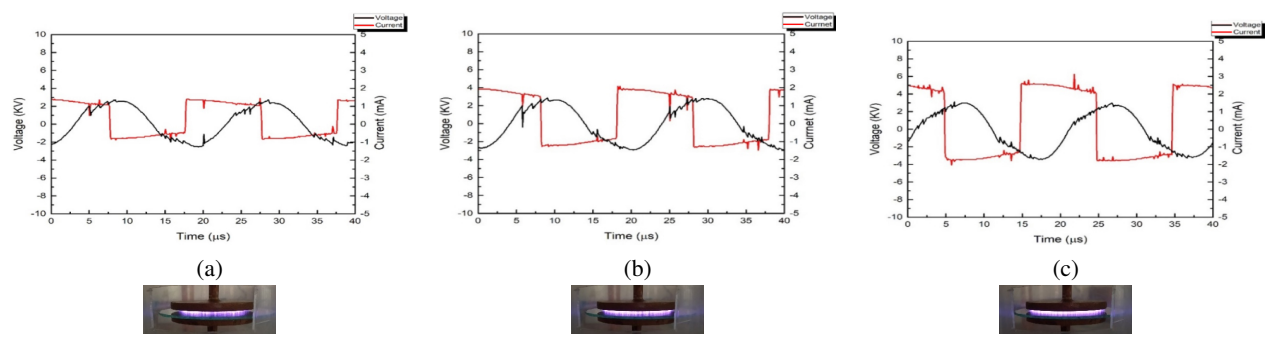


Figure 5. The voltage and current waveforms of disc electrodes in air with a 2mm gap are presented for manually increasing applied voltage. The corresponding photographs of the discharge are placed below.

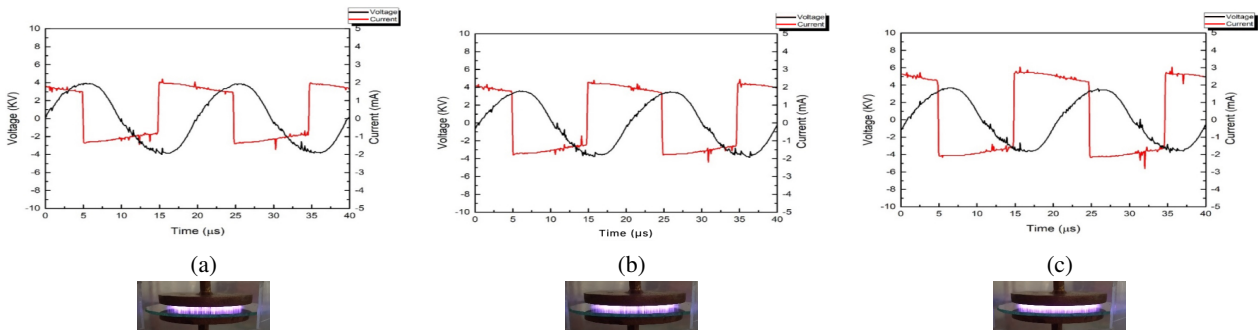


Figure 6. The voltage and current waveforms of disc electrodes in air with a 3mm gap are presented for manually increasing applied voltage. The corresponding photographs of the discharge are placed below.

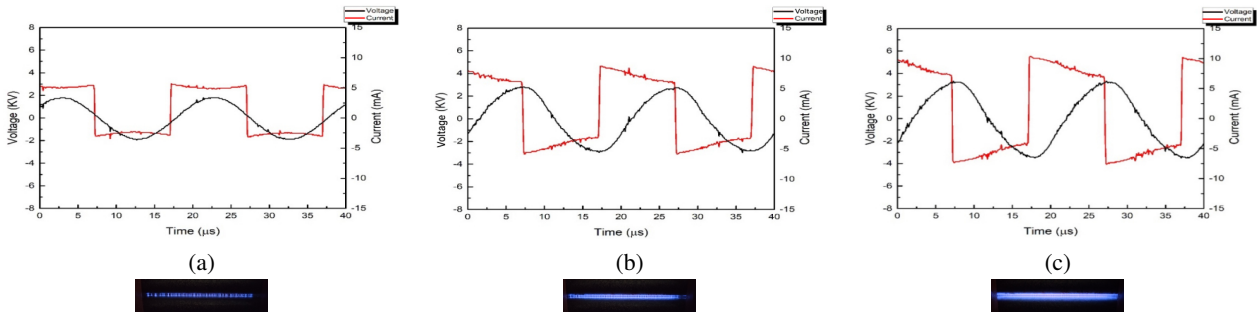


Figure 7. The voltage and current waveforms of cylindrical electrodes in air with a 2mm gap are presented for manually increasing applied voltage. The corresponding photographs of the discharge are placed below.

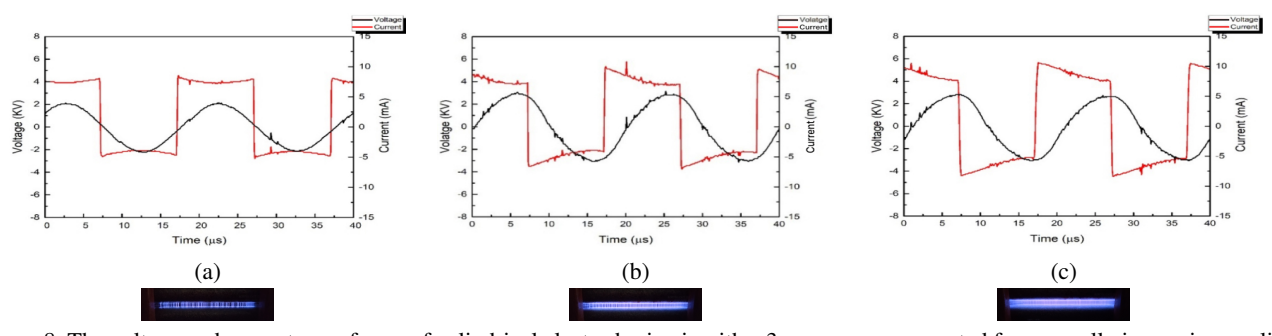


Figure 8. The voltage and current waveforms of cylindrical electrodes in air with a 3mm gap are presented for manually increasing applied voltage. The corresponding photographs of the discharge are placed below.

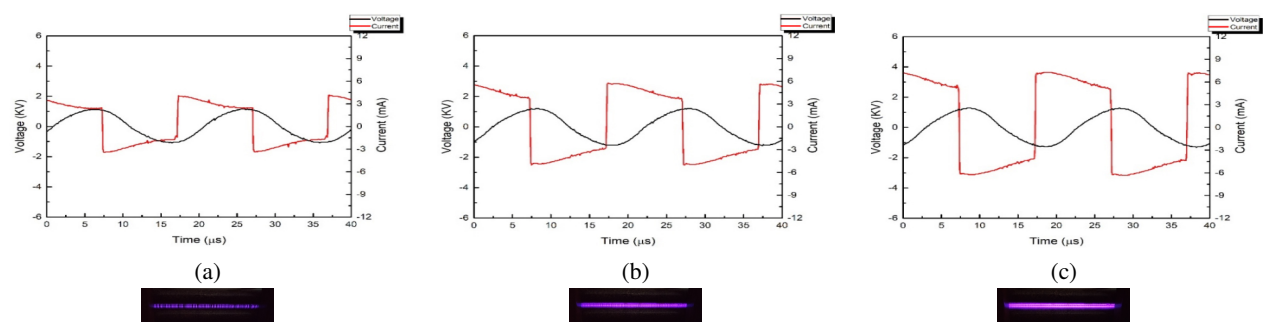


Figure 9. The voltage and current waveforms of double cylindrical electrodes in air with a 2mm gap are presented for manually increasing applied voltage. The corresponding photographs of the discharge are placed below.

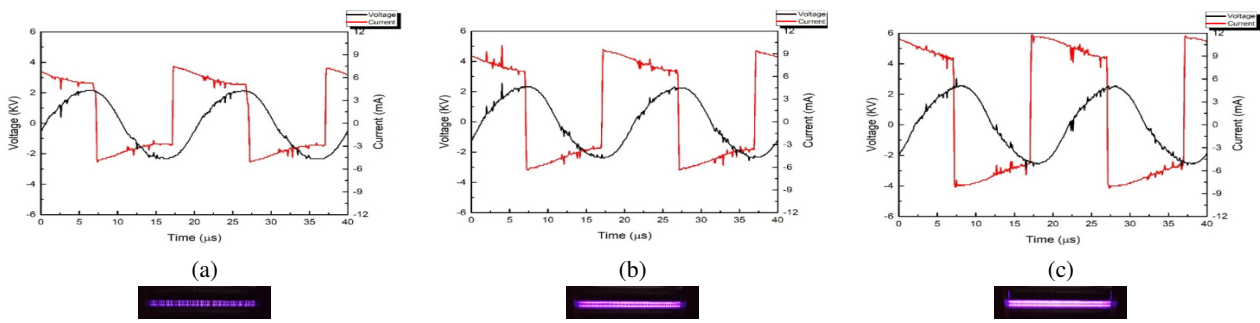


Figure 10. The voltage and current waveforms of double cylindrical electrodes in air with a 3mm gap are presented for manually increasing applied voltage. The corresponding photographs of the discharge are placed below.

3.2. Power Analysis

The mean power consumption for a double cylindrical electrode with a 2 mm gap is one-third that of a single cylindrical electrode with the same gap and is nearly equal to that of a disc electrode with the same gap as shown in Figure 11. The applied voltage differs for each electrode system, increasing until a homogeneous plasma is no longer achieved. This results in overlapping data points.

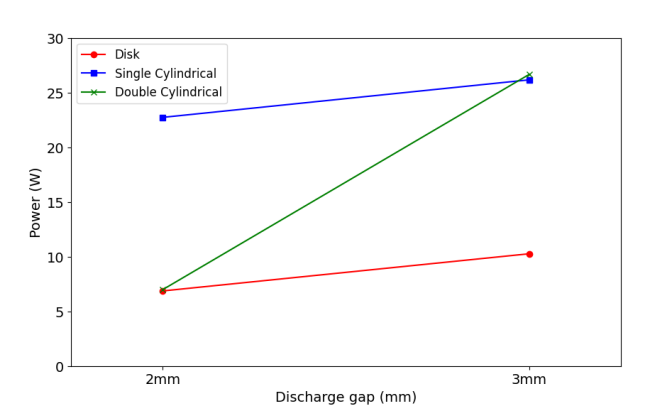


Figure 11. Average pk-pk power comparison of different electrode systems for graphs (a-c) at discharge gaps of 2 mm and 3 mm.

Notably, the double cylindrical electrode with a 2 mm discharge gap successfully sustains a stable glow discharge while consuming only 7.3 W, making it more efficient com-

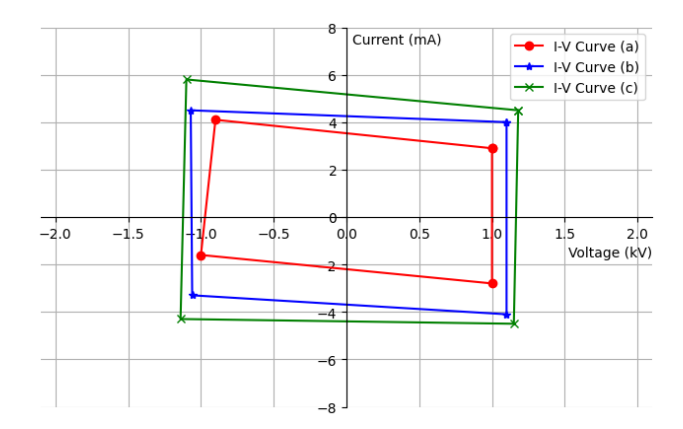


Figure 12. I-V characteristic curve for a double cylindrical electrode system with a 2 mm discharge gap.

pared to the other configurations where stable glow discharges were not achieved.

Shrestha et al. (2013) reported that the discharge current increases with both applied voltage and the discharge gap. This trend is also observed in our experiment. The energy deposition to the discharge, W_{dep} , is calculated as

$$W_{\rm dep} = \frac{\langle P_{\rm dis} \rangle}{2f} \tag{1}$$

where $P_{\rm dis}$ is the average power consumed by the discharge and f is the frequency of the applied source.

Using Equation (1) we calculated that the energy dissipation for a double cylindrical electrode system with a 2mm discharge gap is $18.25 \mu J$.

The four different values for voltage and current in all three cases (a-c) of a double cylindrical electrode system with a 2 mm discharge gap were used to construct Figure 12. The average energy calculated for the same system with a discharge gap of 2 mm from the I-V characteristic curve is 16.74 μ J. Less energy deposition to the discharge was also reported when obtained from the Lissajous plot compared to direct calculation using applied voltage and discharge current (Tyata et al., 2013).

4. Conclusion

This paper studied the electrical characterization of Dielectric Barrier Discharge (DBD) in air at atmospheric pressure using various electrode configurations, including disc, cylindrical, and double cylindrical electrodes. In previous works, the disk electrode system is reported to be more efficient as compared to the single cylindrical system. This study further extended the single cylindrical system to the double cylindrical system. Notably, a stable glow discharge was observed in the double cylindrical electrode system with a 2 mm gap. This configuration is efficient, with the average power consumption being only one-third of that required by the single cylindrical electrode at the same gap.

5. Acknowledgment

We would like to express our sincere gratitude to Khwopa College of Engineering for providing access to their plasma laboratory facilities and the necessary equipment required for this work. We greatly appreciate the continued guidance and support and expertise of the faculty and staff of the college.

References

- Foest, R., Schmidt, M., & Becker, K. (2006). Microplasmas, an emerging field of low-temperature plasma science and technology. *International Journal of Mass Spectrometry*, 248(3), 87–102. https://doi.org/10.1016/j.ijms.2005.11.010
- Jabur, Y. K., Khalaf, M. K., & Hammed, M. G. (2020). A comparative study of the electrical characteristics of generating argon plasma in different interelectrode spacing discharges. *International Journal of Nanoelectronics and Materials*.
- Kogelschatz, U. (2002). Filamentary, patterned, and diffuse barrier discharges. *IEEE Transactions on Plasma Science*, 30(4), 1400–1408. https://doi.org/10.1109/TPS.2002.804201

- Lieberman, M. A., & Lichtenberg, A. J. (1994). Principles of plasma discharges and materials processing. *MRS Bulletin*, 30(12), 899–901.
- Shrestha, P., Subedi, D. P., & Joshi, U. M. (2013). Electrical characterization of atmospheric pressure dielectric barrier discharge in air. *Proceedings of the 5th International Conference on the Frontiers of Plasma Physics and Technology*, 8.
- Siemens, W. (1857). Ueber die elektrostatische induction und die verzögerung des stroms in flaschendrähten. *Annalen der Physik*, 178(9), 66–122.
- Singh, A. K., Guragain, R. P., Shrestha, A., Chhetri, G. K., Dhungana, S., Baniya, H. B., Subedi, D. P., & Joshi, U. M. (2024). Electrical diagnostics of dielectric barrier discharge for optimal power determination. *Journal of Physics Communications*, 8(12), 125003. https://doi.org/10.1088/2399-6528/ad9a38
- Subedi, D., & Tyata, R. B. (2010). An investigation of the effect of electrode geometry and frequency of power supply in the homogeneity of dielectric barrier discharge in air. *Kathmandu University Journal of Science, Engineering and Technology*, *6*(1), 96–101.
- Tyata, R. B., Subedi, D. P., & Wong, C. S. (2010). Comparison of dielectric barrier discharge in air, Nitrogen and Argon at atmospheric pressure. *Kathmandu University Journal of Science, Engineering and Technology*, 6(2), 6–12.
- Tyata, R. B., Subedi, D. P., Shrestha, R., & Wong, C. S. (2013). Generation of uniform atmospheric pressure Argon glow plasma by dielectric barrier discharge. *Pramana*, 80, 507–517. https://doi.org/10.1007/s12043-012-0494-z
- Wang, C., & He, X. (2006). Effect of atmospheric pressure dielectric barrier discharge air plasma on electrode surface. Applied Surface Science, 253(2), 926– 929. https://doi.org/10.1016/j.apsusc.2006.01.032
- Wang, C., Zhang, G., & Wang, X. (2012). Comparisons of discharge characteristics of a dielectric barrier discharge with different electrode structures [Selected papers from the IUVSTA 18th International Vacuum Congress (IVC-18) held in Beijing, P.R.China, 23 -27 August 2010]. *Vacuum*, 86(7), 960–964. https://doi.org/10.1016/j.vacuum.2011.06.027

This work is licensed under a Creative Commons "Attribution-NonCommercial-NoDerivatives 4.0 International" license.

